SEMARAK ILMU PUBLISHING

Journal of Advanced Research in Fluid Mechanics and Thermal Sciences

Journal homepage:
https://semarakilmu.com.my/journals/index.php/fluid_mechanics_thermal_sciences/index
ISSN: 2289-7879

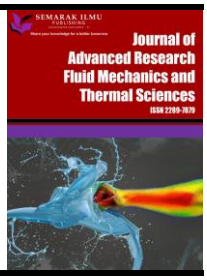

Design of Ocean Current Blade Turbine 100 kW using Hydrodynamics Simulation Approach

Arfie Ikhsan Firmansyah[1,3], Nina Konitat Supriatna[1,*], Bono Pranoto[2,4]

[1] Research Centre for Energy Conversion and Conservation (PRKKE), National Research and Innovation Agency (BRIN), B. J. Habibie Science and Technology Park Bldg. 620, South Tangerang 15314, Province of Banten, Indonesia
[2] Research Center for Geospatial, National Research and Innovation Agency (BRIN), Bogor, Indonesia
[3] Department of Ocean Engineering, Faculty of Marine Technology, Sepuluh Nopember Institute of Technology, Surabaya, Indonesia
[4] Natural Resources and Environmental Management Science (NREMS), IPB University, Bogor, Indonesia

ARTICLE INFO

Article history:
Received 25 May 2022
Received in revised form 27 October 2022
Accepted 10 November 2022
Available online 28 November 2022

Keywords:
Ocean current power plant; location; turbine blade; CFD

ABSTRACT

National electricity consumed continues to rise by up to 6.4 % per year, which are not comparable with the availability of fossil fuels as a primary energy coal-fired power plant in Indonesia. Utilization of ocean energy in particular flow energy has performed as one of the primary energy options. Tides are responsible for the renewable energy of ocean currents. Changes in flow velocity of ocean water due to the ups and downs of ocean water can be used as the primary energy to drive turbines and generate electricity. This study investigates the ocean current power plant in Indonesia that relates to the characteristics of the ocean current. The data used for this research belonged to R&D Center Marine Geology (PPPGL) from ocean current data in the Toyapakeh, Pantar, Larantuka, Molo, Boleng and Gam strait. This study looked at both the technical and socioeconomic aspects of the six locations mentioned above. Larantuka strait had the greatest potential for ocean currents in the strait. The turbine was designed using Computational Fluid Dynamics (CFD), with a capacity of 100 kW for the Horizontal Axis turbine. The findings demonstrated that the turbine design could produce electrical energy at low ocean current speeds (cut-in speed) of 0.3 m/s, and that the rotor power generated at ocean current speeds of 2.2 m/s approached the design capacity of 100 kW.

1. Introduction

National electricity consumed continues to rise by up to 6.4 % per year, are not comparable with the availability of fossil fuels as a primary energy coal-fired power plant in Indonesia [1]. Indonesia is the largest archipelago country in the world, consist of 63 % ocean territory. Ocean has reserved much potential energy, one of that is ocean current [2]. Ocean current has not optimally been utilized for power generation in Indonesia.

The renewable energy of ocean currents was from by tides [3]. Changes in flow velocity of ocean water due to the ups and downs of ocean water could be used as the primary energy to drive turbines

* *Corresponding author.*
E-mail address: nina016@brin.go.id

https://doi.org/10.37934/arfmts.101.1.174185

and generate electricity [4]. There are two types of ocean current turbines, namely Horizontal Axis Turbines (HAT) and Vertical Axis Turbines (VAT) [5,6]. HAT blade was designed as counter ocean current flow, that had kinetic energy from blade spinning by ocean current velocity (Figure 1(a)). VAT blade was design perpendicular ocean current flow (Figure 1(b)).

Numerous articles have discussed the performance of NACA utilizing CFD. Comparing NACA 0010, NACA 2410, NACA 0015, NACA 2412, NACA 0018, NACA 2421, NACA 0021, NACA 4412, NACA 0024, and NACA 4421 on wind turbines using 2D Ansys, Loutun *et al.,* [7] discovered that NACA0018 had the highest power coefficient among all NACA airfoils operating at TSR = 6.2 with a power coefficient of 0.2968795. Using NACA 63-9XX and ANSYS CFX18.0 to simulate a tidal turbine, Wang *et al.,* [8] determined that the greatest power coefficient is 0.45 at TSR = 8. Tian *et al.,* [9], utilizing NACA 63-8xx on a horizontal axis ocean current turbine with ANSYS FLUENT v14.0, got simulated results with a maximum Cp value of 0.38 at a TSR of 5. Guo *et al.,* [10] got a maximum power coefficient of 0.42 at TSR = 5 utilizing bidirectional foil with NACA 65-012 and NACA 65-021 on Tidal Current Turbine with code STAR-CCM+. Using NACA 030 and Fluent on a Horizontal-Axis Tidal Current Turbine, Yan *et al.,* [11] determined a maximum power coefficient of 0.25 at TSR = 4. In this research, it is necessary to choose NACA based on its high Cp and low TSR.

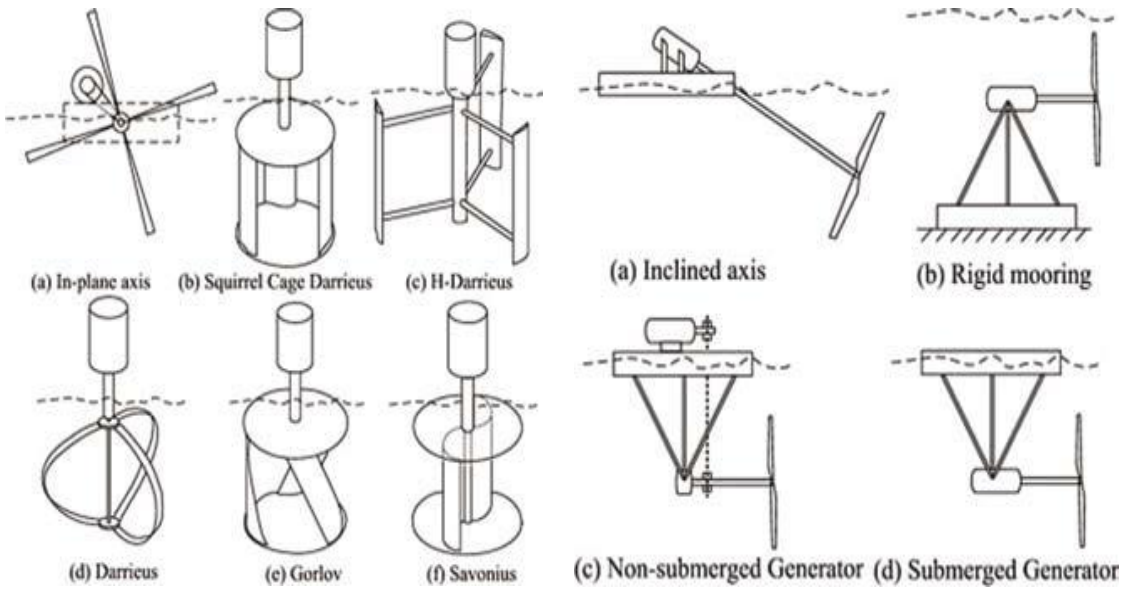

Fig. 1. Ocean current turbines (a) Horizontal axis turbines [5] (b) Vertical axis turbine [5]

The study of ocean current turbine was basic for having turbine blade design. The research aimed to design 100 kW ocean current blade turbine based on a location of ocean current power plant.

2. Methodology

The data on Indonesia ocean currents potential were used PPPGL measurement ocean current data at 6 locations, which had: Toyapakeh Strait, Pantar Strait, Larantuka Strait, Molo Strait, Boleng Strait, Provinsi and Gam Strait. The parametric design of ocean turbine blade was based condition in location selection. The first step to design ocean current blade turbines was calculated swept area of blade turbine has calculate with Betz equation, as follow [12].

$$\frac{P}{A} = \frac{1}{2}\rho V^3 \tag{1}$$

Tip speed ratio of blade turbine determined amount of blade turbine [13]. The equation calculated tip speed ratio, that is

$$\lambda = \frac{2\pi Rn}{60V} \tag{2}$$

where, R is radius ocean current blade, and is generator rotation and V is ocean current speed. Table 1 showed a relation tip speed ratio and the amount of blade turbine [14].

Table 1
Relation tip speed ratio and amount of blade turbine

λ	B
1	6-20
2	4-12
3	3-6
4	2-4
5-8	2-3
8-15	1-2

For this paper, the hydrofoil of the ocean current turbine blade has used NACA 0016. According to previous paper, NACA 0016 is more optimal than NACA 0020 [15]. From the calculation results with NACA 016, with obtained TSR = 3.

NACA airfoil ordinate generation program v 4.5 was used to analyze coefficient lift for NACA shown in Figure 2.

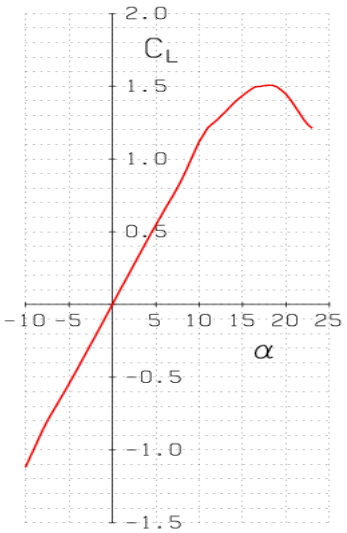

Fig. 2. Coefficient lift NACA 0016 at Re 1424000 with various angle attack

Chord setting of the ocean current blade was done by a separate ocean current blade turbine. The blade size was similar according to Eq. (3).

$$\lambda_r = \frac{\lambda r}{R} \tag{3}$$

From Eq. (3), local speed ratio was calculated for every separate blade. The angle of inclination (Φ) was calculated with Eq. (4) (Figure 3).

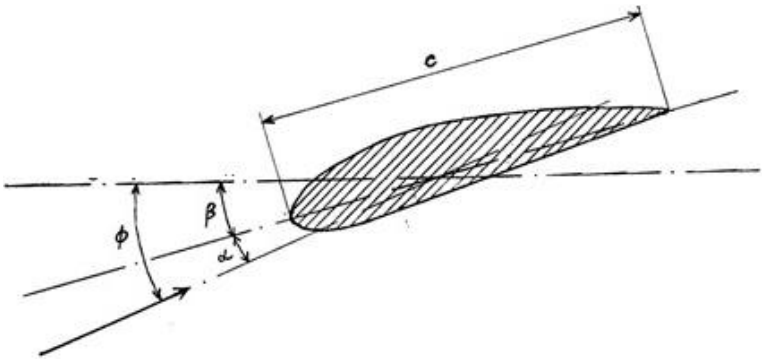

Fig. 3. The angle of inclination (Φ)

$$\Phi = \frac{2}{3}\, arctg\, \frac{1}{\lambda r} \tag{4}$$

The Chord of the blade for every separate ocean current turbine blade was calculated with Eq. (5).

$$\mathrm{c} = \frac{8\pi r}{\mathrm{B\ Cl}} \tag{5}$$

where, B is the total amount of ocean current blade turbine and Cl is the coefficient lift. Angel β for every blade turbine is calculated with Eq. (6). where the angle of attack α is 5 degrees [16].

$$\mathrm{B} = \Phi - \alpha \tag{6}$$

Here is a table of calculation results following the steps above.

Table 2
Initial blade design geometric parameters

Cross-section	r (m)	λr (degrees)	Φ (degrees)	C (m)	B (degrees)
1	0.8	0.69	37.06	0.9	19.06
2	1.6	1.37	24.08	0.78	6.08
3	2.4	2.06	17.03	0.61	-0.70
4	3.2	2.74	13.37	0.48	-4.63

The next step after the design of the ocean current turbine is hydrodynamic simulation. Computational Fluids Dynamic is a method to analyze the hydrodynamic of the ocean current blade turbine [17,18]. The flow chart diagram is shown in Figure 4.

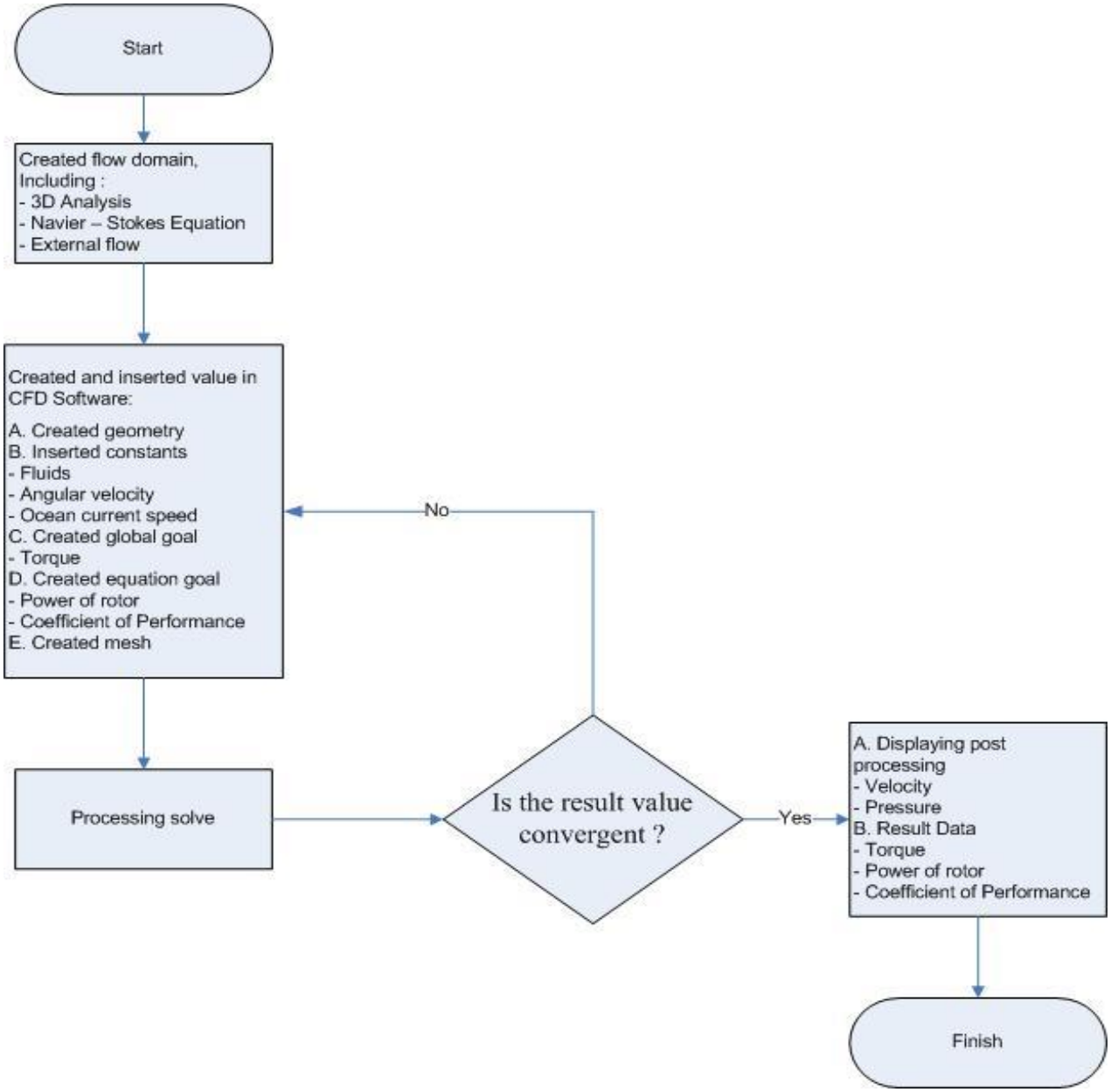

Fig. 4. The flow chart diagram of Computational Fluids Dynamic hydrodynamic of the ocean current blade turbine

To solve discretized fluid flow equations, it is necessary to discretize the computational domain into a computational grid (or mesh). Figure 5 depicts the simulation computational domain for this work.

Torque and force were then calculated by specifying boundary conditions and solving the governing fluid dynamic equations to obtain the pressure and velocity fields within the flow domain. The fluid inlet and outlet velocities were defined as the velocity of the free airstream (V_0).

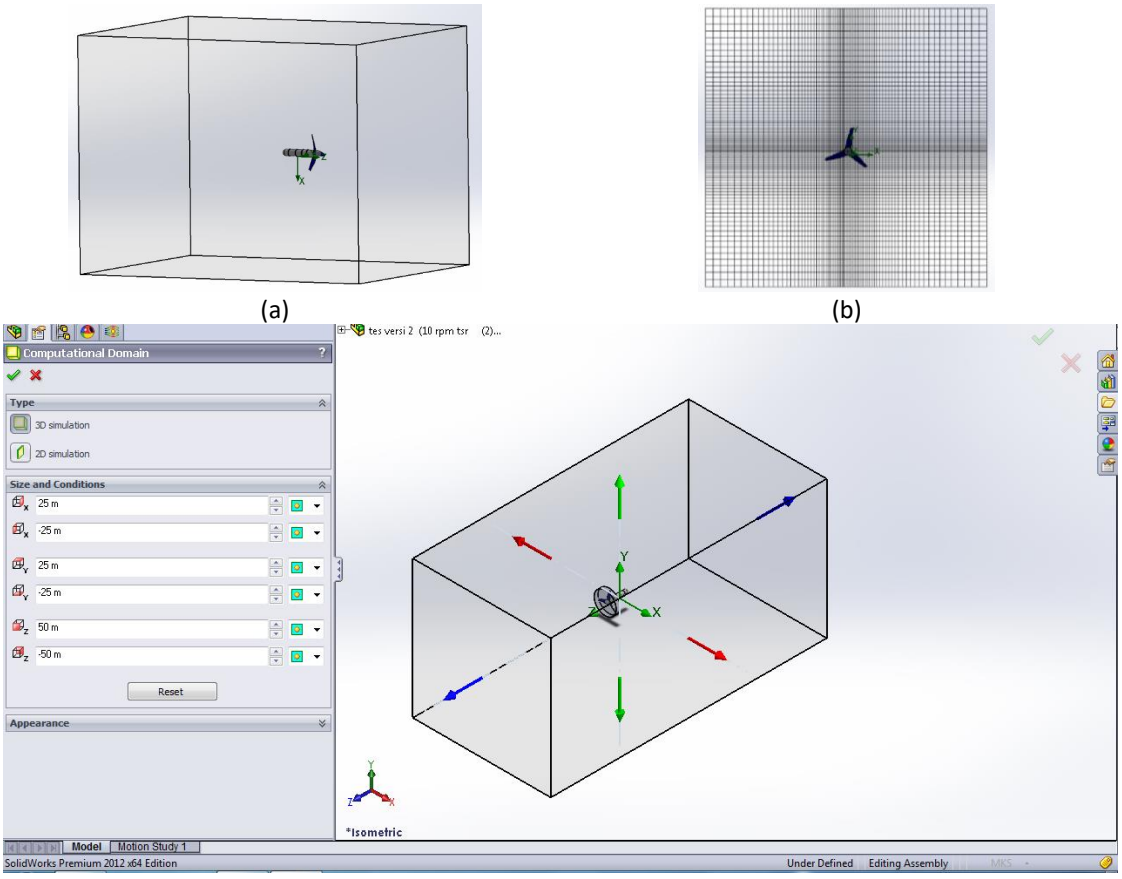

Fig. 5. Three blades in the fluid Domain (a) Front view (b) mesh view (c) computational fluid

Fluid dynamics is the study of fluid motion involving action and reaction forces, i.e., forces that cause acceleration and forces that resist acceleration. The three fundamental principles of mass, momentum, and energy conservation govern the equations that govern the motion of fluids [19,20]. As follow

Continuity equation

$$\frac{\partial \rho}{\partial t} + \nabla.(\rho V) = 0 \tag{7}$$

Navier-Stokes equation

$$\rho \frac{\partial V}{\partial T} + V.\nabla(\rho V) = \nabla.\tau_{ij} - \nabla P + \rho F \tag{8}$$

Energy equation

$$\rho \frac{De}{Dt} + P(\nabla.V) = \frac{\partial Q}{\partial t} - \nabla.q + \Phi \tag{9}$$

where ∇ is $\left(\frac{\partial}{\partial x} + \frac{\partial}{\partial y} + \frac{\partial}{\partial z}\right)$.

An independent grid solution is the objective of a grid dependency analysis. When conducting a new study, it is unlikely that the first grid generated will have the required resolution to capture the flow physics adequately. For this study, a low-resolution initial grid was generated, and then the same meshing scheme was utilized to generate grids with higher resolutions. All simulations for the grid study were performed with the conventional blade (C-Blade) at a current speed of 2.2 m/s, the results are tabulated in Table 3.

Table 3
Grid convergence study

No.	Resolution (cell)	Torque (N x m)	Force (N)
1	52445	1959,4	7112,79
2	62619	2010,9	7112,25
3	74158	4128,44	9062,66
4	88607	4437,6	9012,59
5	102936	4376.92	8967,08

As showed in Table 3, the torque and force vary between the first and third grids but do not change significantly after the third grid. Therefore, the third grid with a resolution of 102936 cells was chosen as the basis for all grids in this study.

3. Results and Discussion

The location selection of Ocean Current power plant was evaluated on the technical aspects and the social economy. The parameter of assessment was made to find the best location. The Parameter of location selection is shown in Table 4.

Table 4
The Parameter of location selection

Variable	Quality	Parameter	Quality	Sub Parameter	Quality
Technical Aspect	0.8	Hydro oceanography	0.3	Maximum Ocean Current Velocity	
				Depth 0-5 m	
				Depth 5-10 m	3
				Depth 5-10 m	
				Minimum Ocean Current Velocity	
				Depth 0-5 m	
				Depth 5-10 m	3
				Depth 10-15 m	
				Average Ocean Current Velocity	
				Depth 0-5 m	
				Depth 5-10 m	4
				Depth 10-15 m	
		Geology	0.1	Formation and Morfology Sea Floor	1
		Seismic Risk	0.1		
		Transmission and Distribution Aspect	0.1	Distance to Distribution Lane	5
				Distance to Substation	5
		Construction Aspect	0.1	The road existence for construction	5
				The road condition	5
		Electrification Ratio	0.3		
Socio-economic aspect	0.2	Population	0.5		
		Location Status	0.5		

The selection of six locations for the ocean current power plant was made based on a study. The Larantuka strait had the potential for ocean currents. The type turbine is Horizontal Axis with a rated capacity 100 kW. The rated ocean current speed in Larantuka Strait was 2.2 m/s with cut-in and cut-out design speeds 0.3 m/s and 4 m/s. According to Eq. (1), the radius of ocean current blade turbine was 3.2 m as shown in Figure 6.

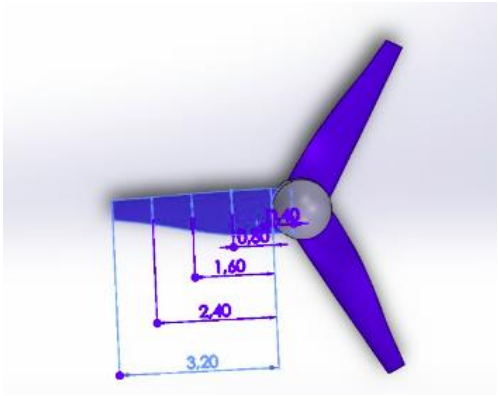

Fig. 6. Dimension of ocean current blade turbine

From Eq. (2), the tip speed ratio (λ) had 6. The relation of the tip speed ratio and amount of blade was described in Table 1, which had total blade turbine 3. The model of the ocean current blade turbine showed Figure 7.

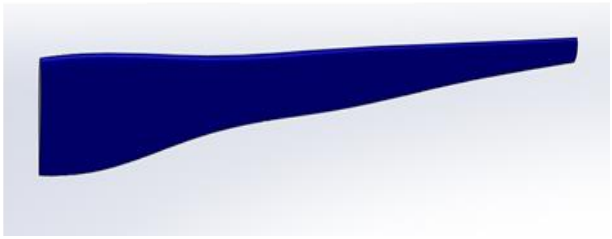

Fig. 7. Model of ocean current blade turbine

Over a variety of rotor thrust coefficients, the performance and wake characteristics of the turbine were determined [21]. The thrust coefficients can be calculated with equation as below.

$$C_T = \frac{T}{0.5\ \rho\ \pi\ A\ {U_T}^2} \tag{10}$$

The variation trend of the energy-harvesting efficiency with increasing TSR at the flow velocity of 2.2 m/s. The energy-harvesting is shown in thrust coefficient obtained by numerical simulation is shown in Figure 8 The overall thrust trend of models increases first and then decreases with the increasing TSR, and the thrust coefficient decreases when TSR is greater than 3.

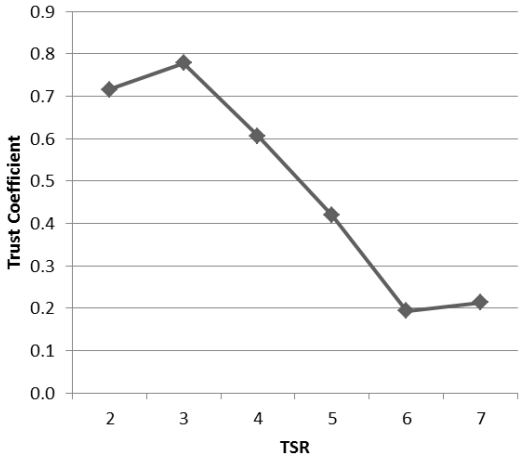

Fig. 8. The overall thrust trend Coefficient with various TSR

The CFD method carried out in this research has been used in previous studies, where the simulation test results compared to the experiment results have a difference with the 1% error standard [15].

The inflow direction power coefficients are defined as follows [22]

$$C_p = \frac{M_x \omega_T}{\frac{1}{2}\rho U^3 \pi R^2} \tag{11}$$

The CFD method research instrument has been utilized in prior studies, where the simulation test results were compared to experiment findings and the simulation power output efficiency was found to be 13% of the power output experienced [15]. The simulation of the power coefficient (Cp) is 12% of the value of the trust coefficient since the trust coefficient or numerical calculation is performed under ideal conditions and the energy loss is minimal. However, the numerical simulation might represent the energy harvesting capability of the turbine in general terms [11]. TSR = 3 produces the highest trust coefficient and Cp simulation, with the TSR adjustment having a significant impact on the operation of the ocean current turbine as shown in Figure 9 [22].

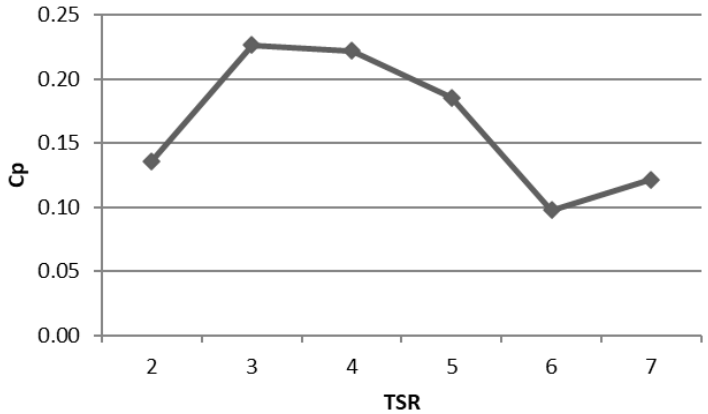

Fig. 9. The overall Cp with various TSR

The result of simulation ocean current blade turbine 100 kW is showed Table 5. According to the findings in Table 5, the turbine's design could create electrical energy at ocean current cut-in speeds as low as 0.3 m/s, and at 2.2 m/s, the rotor power generated attained its design capacity of 100 kW. Figure 10(a) is shown, the visualization of the distribution of pressure on the blade turbine at a

velocity 2.2 m/s with the rotation of the rotor at 18 RPM. Pressure distribution on the surface of each blade turbine has a different value that is due to the different pressure received in turbine geometry. The highest pressure is at the root the of turbine, because it received a larger moment and gravity force [4,23]. Figure 10(b) is shown, flow visualization at an ocean current velocity 2.2 m/s with 18 RPM. The Contour of velocity is shown maximum velocity on the above blade turbine, which makes the blade turbine rotate clockwise. The clockwise rotation of the blade turbine is indicated the design is correct.

Table 5
Simulation CFD Results

Velocity	RPM	Torque	Rotor Power output (kW)	Velocity	RPM	Torque	Rotor Power Output (kW)
0.3	5	406.50	0.24	0.3	30	14937.5	46.93
1.0		757.08	0.40	1.0		14693.2	46.16
1.6		1095.46	0.57	1.6		16218.8	50.28
2.2		1405.46	0.74	2.2		17282.4	53.58
2.6		1741.85	0.91	2.6		18639.6	57.78
3.0		2052.46	1.07	3.0		19648.8	60.91
0.3	15	3569.44	5.61	0.3	35	24296.5	96.68
1.0		4362.04	6.85	1.0		22210.0	88.38
1.6		4895.70	7.69	1.6		24213.8	96.36
2.2		5608.69	8.81	2.2		26651.8	106.06
2.6		6128.74	9.63	2.6		28102.7	111.83
3.0		6771.36	10.64	3.0		28440.9	113.18

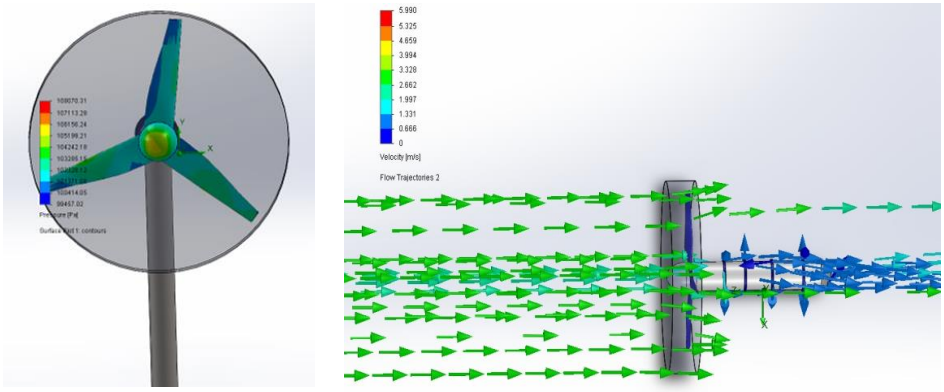

(a) (b)

Fig. 10. (a) Pressure visualization at V = 2.2 m/s, 18 RPM; (b) Flow Trajectory at V = 2.2 m/s

4. Conclusions

Studying the six places' technical characteristics and social-economic aspects have produced The Larantuka Strait has the greatest potential for ocean currents. Computational fluid dynamics (CFD) was used to design the turbine, with a 100 kW horizontal axis turbine capacity. The findings demonstrated that the design of the turbine could generate electrical energy at low ocean current speeds (cut-in speed) of 0.3 m/s and that the rotor power generated at the ocean current speed of 2.2 m/s achieved the design capacity of 100 kW.

Acknowledgement
The author would like to thank The R & D Center Marine Geology (PPPGL) for data support in this research.

References
[1] PT PLN (Persero). "The National Electricity Supply Master Plan 2021-2030." *Jakarta: PT. PLN (Persero)*, 2021.
[2] Li, Ye, Barbara J. Lence, and Sander M. Calisal. "Modeling the Energy Output from an In-Stream Tidal Turbine Farm." *Journal of Computers* 4, no. 4 (2009): 288-294. https://doi.org/10.4304/jcp.4.4.288-294
[3] Rourke, Fergal O., Fergal Boyle, and Anthony Reynolds. "Marine current energy devices: Current status and possible future applications in Ireland." *Renewable and Sustainable Energy Reviews* 14, no. 3 (2010): 1026-1036. https://doi.org/10.1016/j.rser.2009.11.012
[4] Sornes, Kari. "Small-scale water current turbines for river applications." *Zero Emission Resource Organisation (ZERO)* (2010): 1-19.
[5] Khan, Jahangir, and Gouri S. Bhuyan. "Ocean energy: Global technology development status." *Report prepared by Powertech Labs for the IEA-OES* (2009): 83.
[6] Ouro, Pablo, Paul Dené, Patxi Garcia-Novo, Tim Stallard, Yusaku Kyozuda, and Peter Stansby. "Power density capacity of tidal stream turbine arrays with horizontal and vertical axis turbines." *Journal of Ocean Engineering and Marine Energy* (2022): 1-16. https://doi.org/10.1007/s40722-022-00257-8
[7] Loutun, Mark Jason Thomas, Djamal Hissein Didane, Mohd Faizal Mohideen Batcha, Kamil Abdullah, Mas Fawzi Mohd Ali, Akmal Nizam Mohammed, and Lukmon Owolabi Afolabi. "2D CFD Simulation Study on the Performance of Various NACA Airfoils." *CFD Letters* 13, no. 4 (2021): 38-50. https://doi.org/10.37934/cfdl.13.4.3850
[8] Wang, Pengzhong, Bowen Zhao, Haotai Cheng, Bin Huang, Wensheng He, Qiang Zhang, and Fuwei Zhu. "Study on the performance of a 300W counter-rotating type horizontal axis tidal turbine." *Ocean Engineering* 255 (2022): 111446. https://doi.org/10.1016/j.oceaneng.2022.111446
[9] Tian, Wenlong, Xiwen Ni, Zhaoyong Mao, and Tianqi Zhang. "Influence of surface waves on the hydrodynamic performance of a horizontal axis ocean current turbine." *Renewable Energy* 158 (2020): 37-48. https://doi.org/10.1016/j.renene.2020.04.127
[10] Guo, Bin, Dazheng Wang, Xu Zhou, Weichao Shi, and Fengmei Jing. "Performance evaluation of a tidal current turbine with bidirectional symmetrical foils." *Water* 12, no. 1 (2019): 22. https://doi.org/10.3390/w12010022
[11] Yan, Yu-Ting, Shi-Ming Xu, Cong Liu, Xiao Zhang, Jian-Mei Chen, Xue-Ming Zhang, and Yong-Jun Dong. "Research on the Hydrodynamic Performance of a Horizontal-Axis Tidal Current Turbine with Symmetrical Airfoil Blades Based on Swept-Back Models." *Journal of Marine Science and Engineering* 10, no. 10 (2022): 1515. https://doi.org/10.3390/jmse10101515
[12] Buigues, G., I. Zamora, A. J. Mazón, V. Valverde, and F. J. Pérez. "Sea energy conversion: problems and possibilities." In *International Conference on Renewable Energies and Power Quality (ICREPQ'06)*, 8p. 2006. https://doi.org/10.24084/repqj04.242
[13] Lynn, Paul A. *Electricity from wave and tide: an introduction to marine energy*. John Wiley & Sons, 2013. https://doi.org/10.1002/9781118701669
[14] Manwell, James F., Jon G. McGowan, and Anthony L. Rogers. *Wind energy explained: theory, design and application*. John Wiley & Sons, 2009. https://doi.org/10.1002/9781119994367
[15] Firmansyah, Arfie Ikhsan, Bono Pranoto, and Nasruddin Nasruddin. "Kajian Pemanfaatan Energi Arus Laut sebagai Pembangkit Listrik." *Ketenagalistrikan dan Energi Terbarukan* 11, no. 2 (2012): 123-136.
[16] Dajani, S., M. Shehadeh, K. M. Saqr, A. H. Elbatran, N. Hart, A. Soliman, and D. Cheshire. "Numerical Study for a Marine Current Turbine Blade Performance under Varying Angle of Attack." *Energy Procedia* 119 (2017): 898-909. https://doi.org/10.1016/j.egypro.2017.07.143
[17] Gaba, Vivek Kumar, and Shubhankar Bhowmick. "A CFD-based study of cross-flow turbine for tidal energy extraction." In *Sustainable Engineering Products and Manufacturing Technologies*, pp. 177-186. Academic Press, 2019. https://doi.org/10.1016/B978-0-12-816564-5.00007-4
[18] Badshah, Saeed, Mujahid Badshah, Noman Hafeez, Sakhi Jan, and Zia Ur Rehman. "Cfd analysis of tidal current turbine performance with different boundary conditions." In *IOP Conference Series: Earth and Environmental Science*, vol. 581, no. 1, p. 012010. IOP Publishing, 2020. https://doi.org/10.1088/1755-1315/581/1/012010
[19] Kunya, Bashir Isyaku, Clement Olaloye Folayan, Gyang Yakubu Pam, Fatai Olukayode Anafi, and Nura Mu'az Muhammad. "Performance study of Whale-Inspired Wind Turbine Blade at Low Wind Speed Using Numerical Method." *CFD Letters* 11, no. 7 (2019): 11-25.
[20] Ashgriz, Nasser, and Javad Mostaghimi. "An introduction to computational fluid dynamics." *Fluid Flow Handbook* 1 (2002): 1-49.

[21] Karthikeyan, Thandayutham, Lava Kush Mishra, and Abdus Samad. "Optimal Design of a Marine Current Turbine Using CFD and FEA." In *Proceedings of the Fourth International Conference in Ocean Engineering (ICOE2018)*, pp. 675-690. Springer, Singapore, 2019. https://doi.org/10.1007/978-981-13-3134-3_50

[22] Wang, Shu-qi, Chen-Yin Li, Yang-yang Xie, Gang Xu, Ren-qing Zhu, and Kun Liu. "Research on hydrodynamic characteristics of horizontal axis tidal turbine with rotation and pitching motion under free surface condition." *Ocean Engineering* 235 (2021): 109383. https://doi.org/10.1016/j.oceaneng.2021.109383

[23] Jeong, Min-Soo, Myung-Chan Cha, Sang-Woo Kim, In Lee, and Taeseong Kim. "Effects of torsional degree of freedom, geometric nonlinearity, and gravity on aeroelastic behavior of large-scale horizontal axis wind turbine blades under varying wind speed conditions." *Journal of Renewable and Sustainable Energy* 6, no. 2 (2014): 023126. https://doi.org/10.1063/1.4873130